

# The diffuse $\omega$ structure: its relationship to spontaneous vitrification in $\beta$ -Ti–Cr\*

W. Sinkler and D. E. Luzzi

Department of Materials Science and Engineering and the Laboratory for Research on the Structure of Matter, University of Pennsylvania, Philadelphia, PA 19104-6272 (USA)

(Received August 4, 1992; in final form October 19, 1992)

## Abstract

Diffuse scattering from quenched  $\beta$ -Ti–Cr alloys is investigated using electron diffraction. A new structural model based on displacive atomic shifts coupled to chemical short-range order is described and shown to account for the observed diffuse scattering. Changes of the diffuse scattering in  $\text{Ti}_{0.6}\text{Cr}_{0.4}$  due to 1 MeV electron irradiation support the presence of chemical short-range order in quenched Ti–Cr. The significance of these results in light of recent reports that the quenched-in  $\beta$  phase in a concentrated Ti–Cr alloy undergoes a transformation to the amorphous state during low temperature annealing, a process known as spontaneous vitrification, is discussed.

## 1. Introduction

It has been reported [1] that bulk amorphization of a metastable Ti–Cr  $\beta$  (b.c.c.) phase occurs during annealing at approximately 600 °C at compositions between approximately 40 at.% Cr and 55 at.% Cr. The metastable crystalline phase was produced by quenching of the high-temperature  $\beta$  phase of Ti–Cr to room temperature at quenching rates of approximately  $10^3 \text{ K s}^{-1}$ . This report raises the possibility that near-net-shape bulk structures with the novel properties of the amorphous state could be produced using solid state processing routes. However, this bulk amorphous transition, known as spontaneous vitrification (SV), with one exception [2], has not been reproduced despite significant effort by several research groups [3–5]. Successful SV has been reported recently [6] by annealing of  $\beta$ -Cr–Ti, formed by extensive high-energy ball milling (approximately 150 h) of the elemental powders. No extensive investigation has been conducted to date on the metastable  $\beta$  phases prior to annealing.

A feature of the quenched-in metastable  $\beta$  phase is that significant diffuse scattering maxima are seen in electron diffraction patterns. It has been proposed that the appearance of the diffraction pattern may be due to strain in the  $\beta$  phase related to the amorphization [7]. The small grain size of the ball-milled  $\beta$  phase precludes a straightforward determination of the pres-

ence or absence of this diffuse scattering. In a recent study, the distribution of the diffuse scattering in the quenched-in  $\beta$  phase was examined in detail [8]. It was found to bear a one-to-one relationship to the non-b.c.c. reflections seen in b.c.c.-based alloys containing the  $\omega$  phase, with the exception that all diffuse reflections are uniformly shifted with respect to the corresponding reflections of the perfect  $\omega$  phase. A striking feature of the scattering from the quenched-in  $\beta$  phase is the absence of diffuse scattering in diffraction patterns taken with the electron beam along the b.c.c.  $\langle 111 \rangle$  zone axes. A similar absence of diffuse scattering in  $\langle 111 \rangle$ -type diffraction patterns has been seen during irradiation-induced amorphization of  $\text{Cu}_4\text{Ti}_3$  [9] and FeTi and CoTi [10].

In the present paper, the results of the structural analysis of the quenched-in  $\beta$  phase are examined with regard to the implications for SV. First, the diffuse scattering distribution seen in the quenched-in  $\beta$  phase is investigated as a function of Cr content. The systematics of the behavior of the diffuse scattering are related to varying structural features within the  $\beta$  phase. The evolution of the diffuse scattering during low-temperature irradiation is also presented. Relationships between the diffuse scattering, chemical short-range order and SV are then explored.

## 2. Experimental details

Buttons of Ti–Cr with the compositions  $\text{Ti}_{0.87}\text{Cr}_{0.13}$ ,  $\text{Ti}_{0.8}\text{Cr}_{0.2}$ ,  $\text{Ti}_{0.6}\text{Cr}_{0.4}$  and  $\text{Ti}_{0.5}\text{Cr}_{0.5}$  were produced by arc

\*Paper presented at the Symposium on Solid State Amorphizing Transformations, TMS Fall Meeting, Cincinnati, OH, October 21–24, 1991.

melting Cr and Ti (purities, 99.9% and 99.7% respectively). Slices of the alloys, 1–2 mm thick, were quenched directly into water from 1623–1673 K as described in ref. 8. Thin foils for transmission electron microscopy (TEM) were produced by electropolishing using a solution of 1 part 70% perchloric acid, 20 parts methanol and 7 parts butanol [11]. For all four compositions the resulting alloys were single-phase  $\beta$  which exhibited diffuse scattering in TEM.

In separate experiments, TEM thin foils of quenched  $\text{Ti}_{0.6}\text{Cr}_{0.4}$  were irradiated using high-energy electrons and  $\text{Xe}^+$  ions at the high-voltage electron microscope (HVEM)/Tandem facility at Argonne National Laboratory. A helium-cooled stage was used for the irradiation experiments and the temperature measured at the specimen mount was 10–15 K in both experiments. In the electron irradiation experiment, 1 MeV electrons were used at a dose rate of  $4.8 \times 10^{19}$  electrons  $\text{cm}^{-2} \text{s}^{-1}$  up to a total dose of  $5.7 \times 10^{22}$  electrons  $\text{cm}^{-2}$ , which corresponds to approximately 3.5 displacements per atom (d.p.a.). For  $\text{Xe}^+$ , the dose rate was  $1.7 \times 10^{11}$  ions  $\text{cm}^{-2} \text{s}^{-1}$  to a total dose of  $2.04 \times 10^{15}$  ions  $\text{cm}^{-2}$ ; typical ion doses required for low-temperature amorphization of intermetallic compounds are in the region of  $10^{14}$  ions  $\text{cm}^{-2}$  [12]. While some beam heating of the specimen occurred, it is unlikely that it exceeded 30 K [13] and will not have a bearing on the current results.

### 3. Experimental results

Electron diffraction patterns of the four quenched alloys are shown in Figs. 1(a)–1(d) taken along the  $[0\bar{1}1]$  zone axis. In addition to the crystalline reflections which can be indexed according to the  $\beta$  phase b.c.c. crystal structure, several diffuse reflections are seen at positions incommensurate with respect to the  $\beta$  reflections. The ring-like appearance of the diffuse scattering is not of significance, as the rings consist of discrete diffuse maxima and individual portions of the rings arise from different  $\omega$  variants or double diffraction [3]. The diffuse maxima are broadened into disks perpendicular to  $\langle 111 \rangle_{\beta}$ . The orientation of the small dimension of each diffuse peak implies that the scattering originates from regions elongated along the  $\langle 111 \rangle_{\beta}$  axes. By measuring the dimensions of the diffuse maxima and fitting to the  $\frac{\sin^2(Nx)}{\sin^2x}$  formula for diffraction from a finite periodic object, estimates were made of the dimensions of the regions. The correlation length parallel to  $\langle 111 \rangle_{\beta}$  was found to be approximately 14 Å and that perpendicular to  $\langle 111 \rangle_{\beta}$  was found to be approximately 6 Å for the three alloys with  $x_{\text{Cr}} \geq 0.2$ . For  $\text{Ti}_{0.87}\text{Cr}_{0.13}$  both dimensions were approximately double those for the more concentrated alloys. The

size of the regions responsible for the diffuse scattering is much smaller than the grain size of the  $\beta$  phase which is on the order of 1 mm after quenching. Therefore the diffuse scattering must arise from local relaxations within the  $\beta$  phase.

The structural origin of the diffuse scattering was investigated in detail using electron diffraction. As can be seen in Fig. 1, with increasing Cr content the positions of the diffuse maxima uniformly shift parallel to the  $\langle 111 \rangle_{\beta}$  directions in reciprocal space by an amount  $|\Delta|$ , causing the apparent contraction of the rings about their centers. The increasing value of  $|\Delta|$  with Cr content is illustrated in Fig. 2. At low Cr content, the diffuse maxima approach reciprocal space positions given by

$$hkl_{\beta} \pm \frac{1}{3} \langle 111 \rangle$$

which are the positions of the Bragg reflections from four orientation variants of the crystalline  $\omega$  phase. Thus the diffuse scattering bears a one-to-one relationship with the scattering due to the crystalline  $\omega$  phase with each diffuse peak shifted by an amount  $|\Delta|$  which is dependent on composition in the Cr-Ti system. Due to the similarity to the scattering from crystalline  $\omega$ , in the following the structure responsible for the diffuse scattering will be referred to as diffuse  $\omega$ .

The one-to-one relationship between the diffuse  $\omega$  scattering seen in the quenched-in  $\beta$  phase and crystalline  $\omega$  and the monotonic shifting of the diffuse scattering with Cr content imply a relationship between the real space structures. The crystalline  $\omega$  phase is found in quenched Ti-Cr for compositions between 5 at.% and 8 at.% Cr [14] and its structure is shown in Fig. 3. It forms from  $\beta$  by opposing displacements of neighboring pairs of  $(222)_{\beta}$  planes toward their common midpoint, with each collapsed pair being followed by a single undisplaced  $(222)_{\beta}$  plane. In this way an ABAB stacking sequence along  $[111]_{\beta}$  is produced in which A is a single undisplaced  $(222)_{\beta}$  plane and B is a pair of  $(222)_{\beta}$  planes which are concentrically collapsed together along  $[111]_{\beta}$ . The magnitude  $U$  of the displacements which  $(222)_{\beta}$  planes undergo in the case of crystalline  $\omega$  is  $0.5d_{222(\beta)}$  [15], and the atoms in the B plane of  $\omega$  thus all reside at the same height along  $[111]_{\beta}$ . The periodicity or repeat distance of the crystalline  $\omega$  structure is triple that of the fundamental  $(222)_{\beta}$  plane spacing, and the presence of  $\omega$  precipitates in the  $\beta$  phase thus results in  $(001)\omega$  and  $(002)\omega$  diffraction spots at  $\frac{1}{3}$  and  $\frac{2}{3}$  of the  $(222)_{\beta}$  reciprocal lattice vector  $k_{222(\beta)}$  as well as the other peaks. A feature of the crystalline  $\omega$  structure which is of importance for the following discussion of diffuse  $\omega$  is that it forms from b.c.c. through an ordered set of displacements of entire  $[111]_{\beta}$  atomic columns along their length. This is consistent with the absence of extra peaks in  $\langle 111 \rangle_{\beta}$  zone axis diffraction patterns which is the common signature of b.c.c. lattice distortions as discussed in Section 1. Thus, as can be seen from Fig. 3, in the

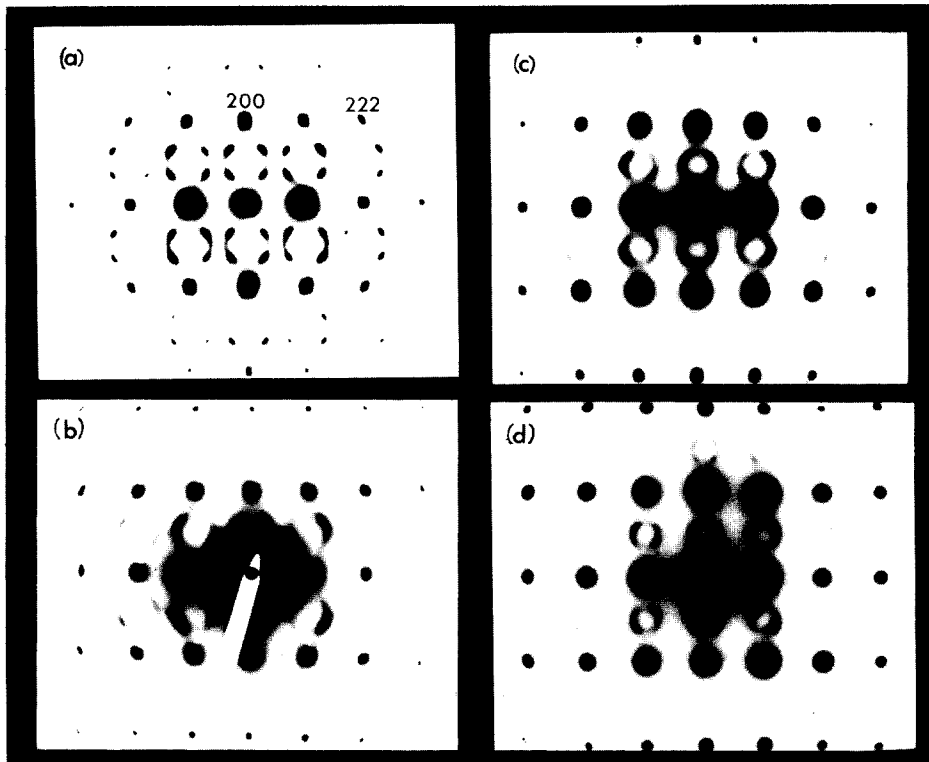


Fig. 1. Quenched Ti-Cr  $[0\bar{1}1]\beta$  zone axis diffraction patterns: (a)  $Ti_{0.87}Cr_{0.13}$ ; (b)  $Ti_{0.8}Cr_{0.2}$ ; (c)  $Ti_{0.4}Cr_{0.6}$ ; (d)  $Ti_{0.5}Cr_{0.5}$ .

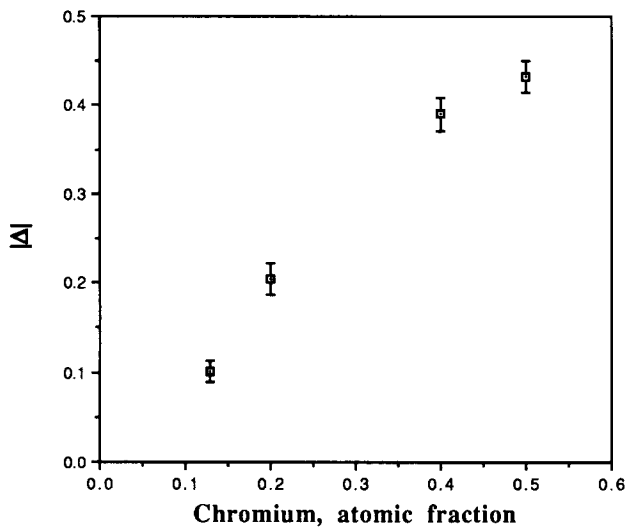


Fig. 2. The magnitude  $|\Delta|$  of the shift of the diffuse maxima from the Bragg positions of the  $\omega$  phase, measured from Fig. 1 and plotted vs. Cr content.

transition from  $\beta$  to crystalline  $\omega$  there are no relative displacements of atoms within the displaced  $[111]\beta$  close-packed atomic columns.

In a detailed analysis to be published elsewhere [8], it was shown that the shifts of the diffuse peaks seen in the quenched  $\beta$  alloys can be reproduced by a structure which is similar to the  $\omega$  phase in that it consists of undisplaced  $(222)\beta$  planes (A planes) and

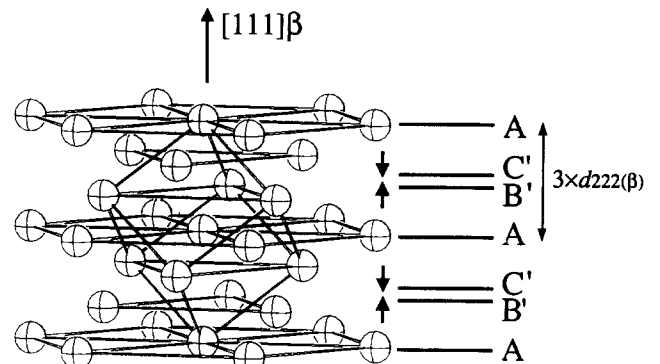


Fig. 3. The formation of the  $\omega$  phase from the b.c.c. lattice:  $\omega$  is formed when the atoms in planes B' and C' move up and down respectively to coincide midway between planes A, forming a B plane. This may also be viewed as a rigid displacement of  $\frac{1}{2}$  of the  $\langle 111 \rangle\beta$  close-packed atomic columns along their length.

pairs of concentrically displaced  $(222)\beta$  planes (B planes). However, in order to reproduce the shift of the diffuse peaks, it is necessary to introduce periodicities other than  $3d_{(222)\beta}$  in the diffuse  $\omega$  structure. The structural feature which is responsible for the displacements of the diffuse peaks in the case of diffuse  $\omega$  scattering was found to be an increase in the average number of consecutive B planes from unity (the number in the  $\omega$  phase) toward larger values [8]. In addition, the A planes in the structure are never nearest neighbors, and tend to be self-avoiding.

Increasing the probability of two or more consecutive B planes destroys the long-range periodicity of the  $\omega$  phase. The sequence of displacements along  $\langle 111 \rangle \beta$  close-packed atomic columns is thus altered from the case of rigid displacements of entire columns along their length. It is found that the diffuse  $\omega$  structure reversals in the direction of atomic displacement must occur along  $\langle 111 \rangle \beta$  close-packed atomic columns as shown in Fig. 4. These consist on average of an equal number of expansive and contractive reversals, the latter of which result in displacements of nearest neighbor atoms toward each other within a single  $\langle 111 \rangle \beta$  atomic column. The presence of reversals in the direction of atomic displacement along  $\langle 111 \rangle \beta$  close-packed atomic columns in diffuse  $\omega$  requires a reduction in the magnitude of the atomic displacement as the solute content is increased in the  $\beta$  phase. This is consistent with previous X-ray diffraction results in the Zr-Nb system which showed that the magnitudes of atomic displacements in the quenched-in  $\beta$  phase containing diffuse  $\omega$  are smaller than those in the crystalline  $\omega$  phase (*i.e.*  $U < 0.5k_{222(\beta)}$ ) [16]. This is also consistent with the observed reduction in overall intensity of the diffuse reflections with increasing Cr content which results in a longer exposure time necessary to record the diffuse scattering at higher Cr contents (see Fig. 1).

The collapse of  $(222)\beta$  planes resulting in B planes is thus only partial in the quenched-in  $\beta$  phase, and such partially collapsed pairs of  $(222)\beta$  planes will be referred to as  $B_p$  planes. A calculated trace from an array in which the average number of consecutive  $B_p$  planes is 1.36 is shown in Fig. 5. From the figure it can be seen that diffuse maxima reside at  $0.35k_{222(\beta)}$  and  $0.65k_{222(\beta)}$ , or  $|\Delta| = 0.24$ , in agreement with the  $[111]\beta$  diffraction trace for the  $\text{Ti}_{0.8}\text{Cr}_{0.2}$  alloy. For the calculations, the magnitude of the displacement of  $(222)\beta$  planes used was  $U = 0.2d_{222(\beta)}$ . Calculated diffractions from arrays in which the average numbers of consecutive  $B_p$  planes are 1.96 and 2.14 reproduce the large displacements of diffuse maxima seen in quenched

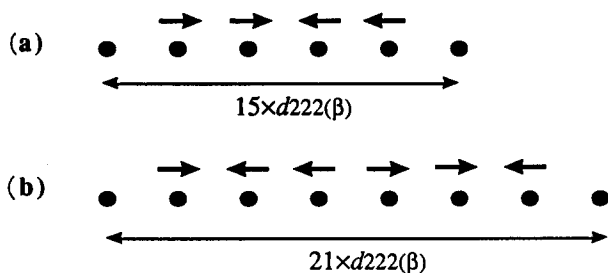


Fig. 4. The sequence of the displacements of atoms along  $\langle 111 \rangle \beta$  columns when the number of consecutive  $B_p$  planes is 2 (a) and 3 (b) (note that the density of reversals in the direction of atomic displacement will increase with the average number of consecutive  $B_p$  planes).

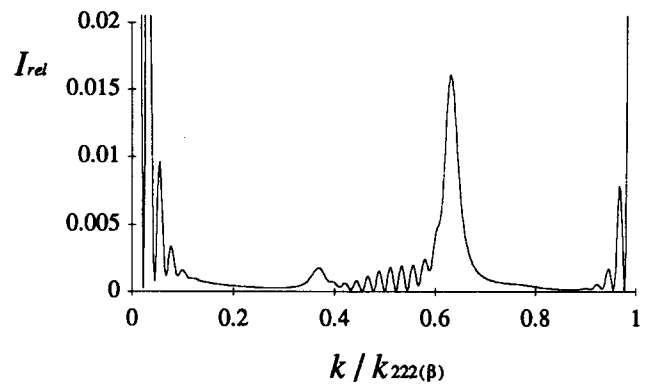


Fig. 5. Calculated diffraction trace along  $\langle 111 \rangle \beta$  for an average number of consecutive  $B_p$  planes of 1.36. The positions of the diffuse maxima match those for the  $\text{Ti}_{0.8}\text{Cr}_{0.2}$  alloy.

$\text{Ti}_{0.6}\text{Cr}_{0.4}$  and  $\text{Ti}_{0.5}\text{Cr}_{0.5}$  respectively [8]. The increase in the average number of consecutive  $B_p$  planes and the presence of conflicting atomic displacements in single  $[111]\beta$  atomic columns are thus central features of the structural evolution with Cr content of the quenched-in  $\beta$  phase in the Ti-Cr alloy system.

Within an atomic column near a reversal, the atomic displacement magnitude is constrained to be small, due to atomic size considerations. In the present structural model the magnitude of  $|\Delta|$  (the diffuse peak shift) was found to be directly proportional to the density of reversals in the direction of displacement along  $[111]\beta$  close-packed atomic columns. The nearly linear increase in  $|\Delta|$  with Cr content in Fig. 2 thus strongly suggests that these reversals are related to the increase in the number of smaller Cr atoms in the alloy. It also suggests that some local ordering of the chemical species may be present in the quenched  $\beta$ . This chemical short-range order (CSRO) would support an increasing number of  $B_p$  planes as well as the self-avoidance of the A planes.

The possibility that some CSRO exists in the nominally disordered quenched solid solution was tested using low-temperature irradiation. It is well known [17] that high-energy, low-temperature irradiation causes a reduction in CSRO in metallic alloys. Irradiation of  $\text{Ti}_{0.6}\text{Cr}_{0.4}$  at low temperature did not result in amorphization of the alloy even after extensive damage by the heavy ions. The results support the existence of some CSRO in the quenched alloy. They are illustrated in Fig. 6 for the case of electron irradiation. As may be seen, the  $(001)\omega$  and  $(002)\omega$  diffuse peaks, which reside between the origin and the  $\langle 222 \rangle \beta$  diffraction peaks, were shifted apart due to the effect of irradiation. Prior to irradiation the diffuse peaks appear at  $0.4k_{222(\beta)}$  and  $0.6k_{222(\beta)}$ , and during irradiation they are shifted to the positions  $0.37k_{222(\beta)}$  and  $0.63k_{222(\beta)}$ , giving a 43% reduction in  $|\Delta|$ . This result is consistent with an irradiation-induced decrease in the average number of

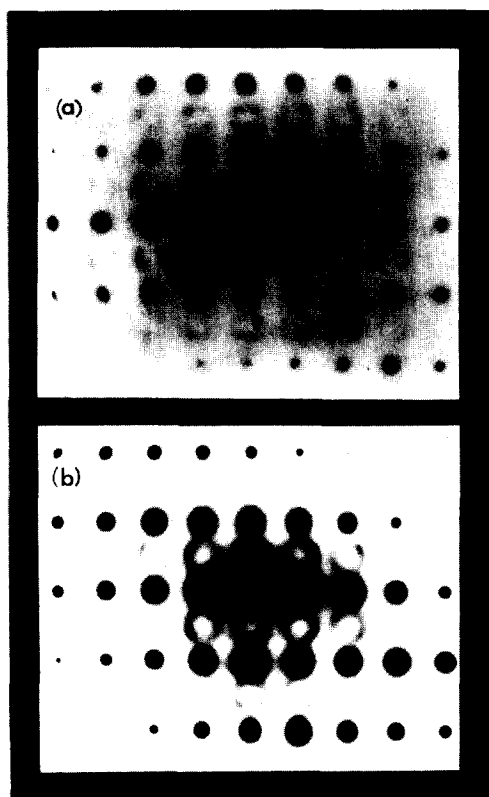


Fig. 6.  $[0\bar{1}1]\beta$  zone axis patterns of  $Ti_{0.4}Cr_{0.6}$  taken prior to irradiation (a) and after 1 MeV electron irradiation at nominally 10 K to a dose of  $5.7 \times 10^{22}$  electrons  $cm^{-2}$  (approximately 3.5 d.p.a.) (b).

consecutive  $B_p$  planes which could be related to a decrease in CSRO in the alloy. An intriguing result of the irradiation experiment is that the diffuse scattering remained, although shifted. This implies that the diffuse  $\omega$  regions remained similar in size during irradiation and that local atomic shifts are not solely the result of CSRO.

#### 4. Discussion

The  $\beta$  phase retained after solid state quenching is not perfect b.c.c. The diffuse scattering seen in electron diffraction patterns indicates the presence of local nanometer-sized regions of relaxation which are columnar in shape. This is consistent with previous TEM imaging studies [18, 19] which relate the disk-like shape of diffuse  $\omega$  maxima to the morphology of diffuse  $\omega$  regions. This morphology was found to be columnar with the column axis either parallel to the  $\omega$   $c$  axis or slightly slanted with respect to this direction [19].

The diffuse scattering distributions seen in electron diffraction patterns of the quenched-in  $\beta$  phase indicate that, within a diffuse  $\omega$  region, atoms are shifted from b.c.c. lattice sites along a single b.c.c.  $[111]$  direction.

It is reasonable to assume that atomic shifts which reduce the interatomic distance along  $\langle 111 \rangle$  are related to the smaller Cr atom. The extra diffuse peaks must therefore be related to the presence of displaced short-range order in the diffuse  $\omega$  regions. The correlation of the magnitude of  $|\Delta|$  with Cr content provides strong evidence that the short-range order is related to the distribution of Cr atoms, *i.e.* chemical short-range order (CSRO).

The structural model [8] indicates that the value of  $|\Delta|$  is linked to the lineal density of  $B_p$  planes in the diffuse  $\omega$  region which is, in turn, a product of the Cr and Ti atom distribution. Under the chemical disordering effect of low-temperature irradiation, the local distribution of Cr atoms conducive to the formation of consecutive  $B_p$  planes would be disturbed, thereby reducing the average number of consecutive  $B_p$  planes in the alloy. Based on the model, this would reduce the value of  $|\Delta|$ ; this is indeed what occurs. Further support for this is provided by the presence of diffuse  $\omega$  scattering with  $|\Delta| \approx 0$  in a Zr-1.5at.%Co alloy at high temperature [20]. In this alloy, Co-Co correlations will be minimal. Additional support for the existence of CSRO in concentrated quenched Ti-Cr is found in an earlier report of annealing-induced transformations in  $Ti_{0.6}Cr_{0.4}$  [3]. On annealing at 600 °C no measurable displacement of diffuse  $\omega$  maxima (*i.e.* no change in  $|\Delta|$ ) was observed. This suggests that the type of CSRO responsible for the appearance of diffuse  $\omega$  scattering in these alloys may have already reached a saturation level in the quenched state.

The experimental evidence indicates that the diffuse  $\omega$  scattering is not a precursor to amorphization in quenched  $\beta$ -Cr-Ti. Rather, the quenched-in  $\beta$  phase has reached a metastable minimum energy state through the formation of one-dimensional displacement fields associated with CSRO. This local collapse occurs in one dimension presumably due to the well-known softness of the b.c.c. lattice to longitudinal distortions parallel to its  $\langle 111 \rangle$  directions [21] coupled with the smaller atomic size of the Cr atoms. On irradiation, diffuse peak shifts will decrease as the CSRO is reduced. However, even in the completely disordered alloy, diffuse scattering will arise due to the softness of the b.c.c. lattice. Therefore, it is not surprising that irradiation does not completely remove the diffuse scattering.

As mentioned in Section 1 amorphization by annealing of the ball-milled Cr-Ti  $\beta$  phase has been reported [6]. On first inspection, this appears to be contradictory to the present observation that no crystalline to amorphous transition occurs in  $Ti_{0.6}Cr_{0.4}$  on high-energy irradiation, which suggests that the Ti-Cr  $\beta$  phase is very stable. In addition, previously reported results indicate that, at the composition of the Laves compound

TiCr<sub>2</sub>, the stable phase on low-temperature irradiation is also the  $\beta$  phase [22, 23]. However, these results are not necessarily inconsistent with the reports of SV, as they merely indicate that as long as chemical ordering is inhibited by a disordering process,  $\beta$  is the most stable phase for all compositions  $x_{Cr} > 8$  at.% in the Ti-Cr system. This is consistent with the result of Yan *et al.* [6] that ball milling of Ti-Cr results in single-phase  $\beta$  alloys at compositions between 40 at.% and 60 at.% Cr. This also supports a previous suggestion that the amorphous phase in the Cr-Ti system is stabilized with respect to  $\beta$  by an increase in CSRO [24].

Assuming that SV of the ball-milled  $\beta$  phase can occur, it is necessary to explain why the  $\beta$  lattice cannot also support an increase in CSRO. This increase in CSRO in the b.c.c. lattice should be easily able to occur at 500–600 °C and would not require nucleation. The observation by Yan *et al.* [6] that grain growth occurs prior to amorphization in ball-milled  $\beta$  indicates that there is sufficient opportunity for this increase of CSRO in the  $\beta$  phase. This implies the existence of a fundamental barrier towards decreasing the free energy of the  $\beta$  phase through an increase in CSRO. If this is the case, this barrier is an underlying factor in the occurrence of SV.

The observation of SV in ball-milled  $\beta$  and not in quenched  $\beta$  may not be a problem of driving force, but rather one of nucleation. In the quenched  $\beta$ , the grain size of 1 mm does not provide sufficient locations for nucleation for the amorphous phase to grow to a sufficient volume fraction prior to the nucleation and growth of the equilibrium phases. In the ball-milled material, a grain size of 100–300 Å provides copious nucleation sites and therefore a complete transformation is observed. Although the present experiments cannot support or refute the occurrence of SV in ball-milled Cr-Ti, this and previous work can place constraints on the composition ranges over which it can occur. Previous experiments have found that the amorphous phase at the TiCr<sub>2</sub> composition crystallizes close to room temperature [23, 25]. The composition TiCr<sub>2</sub> thus lies outside any  $T_0$  curve for amorphous phase stability relative to  $\beta$  in the absence of compositional segregation, a factor which should be considered in thermodynamic modeling.

#### Acknowledgments

This research was funded by the NSF-MRL program through grants DMR-88-19885 and DMR-91-20668. Ad-

ditional support was received from the University of Chicago, Argonne National Laboratory user assistance program. The authors acknowledge stimulating discussions with Professor T. Egami and Dr. C. W. Allen. The authors wish to thank Mr. E. Ryan and Mr. S. Ockers for their assistance at the Argonne HVEM/Tandem facility.

#### References

- 1 A. Blatter, M. von Allmen and N. Baltzer, *J. Appl. Phys.*, **62** (1987) 276.
- 2 Y.-G. Kim and J.-Y. Lee, *J. Non-Cryst. Solids*, **122** (1990) 269.
- 3 W. Sinkler and D. E. Luzzi, in M. J. Aziz, H. B. Stephenson and D. Cherns (eds.), *Mater. Res. Soc. Symp. Proc.*, **205** (1991) 209.
- 4 R. Prasad, R. E. Womekh and A. L. Greer, *Mater. Sci. Eng. A*, **133** (1991) 606.
- 5 K. Ohsaka, E. H. Trinh, J. C. Holzer and W. L. Johnson, *Appl. Phys. Lett.*, **60** (1992) 1079.
- 6 Z. H. Yan, T. Klassen, M. Michaelson, M. Oehring and R. Bormann, *Phys. Rev. B*, submitted for publication.
- 7 A. Blatter, J. Gfeller and M. von Allmen, *J. Less-Common Met.*, **140** (1988) 317.
- 8 W. Sinkler and D. E. Luzzi, *Acta Metall. Mater.*, submitted for publication.
- 9 D. E. Luzzi, *J. Mater. Res.*, **6** (1991) 2056.
- 10 M. Meshii, *Fall Meeting of TMS, Cincinnati, OH, 1991*.
- 11 M. J. Blackburn and J. C. Williams, *Trans. AIME*, **239** (1967) 287.
- 12 C. W. Allen, personal communication, 1992.
- 13 D. E. Luzzi, *Ph.D. Dissertation*, Northwestern University, 1986, Appendix A.
- 14 Y. A. Bagaryatskii and G. I. Nosova, *Phys. Met. Metallogr.*, **13** (1962) 92.
- 15 S. K. Sikka, Y. K. Vohra and R. Chidambaram, *Prog. Mater. Sci.*, **27** (1982) 245.
- 16 W. Lin, H. Spalt and B. W. Batterman, *Phys. Rev. B*, **13** (1976) 5158.
- 17 S. Banerjee, K. Urban and M. Wilkens, *Acta Metall.*, **32** (1984) 299.
- 18 T. S. Kuan and S. L. Sass, *Philos. Mag.*, **36** (1977) 1473.
- 19 D. Schryvers and L. E. Tanner, *Mater. Sci. Forum*, **56–58** (1990) 329.
- 20 A. Heiming, W. Petry, G. Vogl, J. Trampenau, H. R. Schober, J. Chevrier and O. Schärpf, *Z. Phys. B*, **85** (1991) 239.
- 21 C. Falter, W. Ludwig, M. Selmke and W. Zierau, *Phys. Lett. A*, **90** (1982) 250.
- 22 C. W. Allen, L. E. Rehn and H. Wiedersich, *Appl. Phys. Lett.*, **50** (1987) 1876.
- 23 W. Sinkler, D. E. Luzzi and C. W. Allen, *Scripta Metall.*, submitted for publication.
- 24 A. L. Greer, *J. Less-Common Met.*, **140** (1988) 327.
- 25 C. W. Allen and L. E. Rehn, *Ultramicrosc.*, **30** (1988) 188.